Nonreciprocal sound propagation in space-time modulated media

Junfei Li,[1] Chen Shen,[1] Xiaohui Zhu,[2] Yangbo Xie,[1] and Steven A. Cummer[1,*]
[1]*Department of Electrical and Computer Engineering, Duke University, Durham, North Carolina 27708, USA*
[2]*School of Mechatronics Engineering, Harbin Institute of Technology, Harbin 150001, China*

(Received 24 October 2018; revised manuscript received 13 April 2019; published 25 April 2019)

Realization of nonreciprocal devices, such as isolators and circulators, is of fundamental importance in microwave and photonic communication systems. This can be achieved by breaking time-reversal symmetry in the system or exploiting nonlinearity and topological effects. However, exploration of nonreciprocal devices remains scarce in acoustic systems. In this work, sound propagation in a space-time modulated medium is theoretically studied. Finite-difference time-domain simulations are carried out to verify the results. Functionalities such as mode conversion, parametric amplification, and phase conjugation are demonstrated.

DOI: 10.1103/PhysRevB.99.144311

I. INTRODUCTION

Reciprocity is a fundamental principle for most wave systems in which the relationship between a source at one point and the measured response at another point is symmetric when the source and measurement points are interchanged. For a long time, nonreciprocal devices that break this symmetry have been pursued since there are many practical situations where breaking reciprocity can be advantageous. In electric circuits, nonreciprocity can easily be achieved through nonlinear semiconductor devices, and diodes and transistors are widely used in almost all electronic systems. For optics and electromagnetics, nonreciprocity has been demonstrated using magnetic field biasing [1], nonlinearity [2,3], systems with angular momentum bias [4], and topological insulators [5–7]. Despite the growing interest in nonreciprocity in optics and electromagnetics in recent years, nonreciprocal phenomena and devices for acoustic waves are less explored [8].

For acoustic systems, nonreciprocity has been primarily achieved through nonlinear effects that partially convert the energy in fundamental modes into higher harmonics and applying spatial or temporal frequency filters [9–12]. However, nonlinear effects are weak for most materials, and the amplitude needs to be impractically high to induce significant nonlinear effects. Also, it is difficult to have full control over the spectrum through nonlinear effects because of the generation of many harmonics in these systems. Another approach is to introduce directional bias by constant air flow [13]. However, this approach requires mechanical motion that is associated with high-energy consumption, which can create challenges for device-based implementations. In recent years, topological insulators that break reciprocity with external bias, such as constant flow or directional modulation, have also attracted much attention [14–17]. However, such systems require sophisticated control of the flow field or multiple coupled resonances that are sensitive to losses, making them hard to implement in experiments.

Breaking time-reversal symmetry using space-time modulation has been studied in time-varying transmission lines for many decades [18–26]. Recently, nonreciprocity through space-time modulation has returned to the spotlight, and the idea has been applied to modern optical and electromagnetic systems and metasurfaces [27–35]. For mechanical waves, space-time modulated elastic beams have been proposed to create a directional band gap [36]. Space-time modulated waves in mass-spring systems have also been proposed to create directional wave manipulation for elastic waves [37,38]. For acoustics, time modulated circulators have been studied using coupled-mode theory [39,40].

In this paper, acoustic wave propagation in a general space-time modulated medium is studied by directly solving the time-varying wave equations instead of using time Floquet theory [41] to analyze its band gaps. This is because the Floquet theory is not applied to our scenario due to the particular material modulation, which will be further explained in the following section. We follow an approach originally applied to a time-varying transmission line system [19]. For such a system, two otherwise orthogonal waveguide modes can be coupled efficiently under certain conditions, giving rise to interband and intraband phonon transition. Instead of using time Floquet theory, we directly solve the equations to provide full and detailed information on how propagating waves change gradually in such a system. By applying different types of modulation, different nonreciprocal functionalities can be achieved, including one-way frequency conversion, parametric amplification, and phase conjugation. Modulation conditions under which each of these behaviors emerge are derived, and finite-difference time-domain (FDTD) simulations of the full dynamical system show good agreement with the theoretical predictions. The proposed approach for breaking time-reversal symmetry can find applications in numerous areas that leverage the resulting unprecedented wave control capability. For example, mode conversion enables directional band gap for acoustic waves [36], rectifiers [9], and advanced spectrum control for communication and energy transmission [42]; parametric amplification provides a possible implementation for the gain media in parity-time-symmetric systems

*cummer@ee.duke.edu

[43] and powerful speaker designs; and phase conjugation can be useful for an all-angle retroreflector, acoustic lasing [44,45], imaging [46], data processing, and acoustic communications [45].

II. NONRECIPROCAL SOUND PROPAGATION THROUGH SPACE-TIME MODULATED MEDIA

In this section, we will start with solving the space-time-varying wave equation and investigate the acoustic wave propagation in a medium whose density varies with both space and time, as is shown in Fig. 1. A similar coupled wave solution can be found in [18], where two transmission lines are coupled with varying inductors, while in our paper we focus on acoustic wave propagation in one waveguide. We will show that by applying specific types of modulation, two otherwise orthogonal waves will be coupled, and phenomena like frequency conversion and parametric amplification will arise. Then we will show that these phenomena will also arise when the bulk modulus is modulated the same way. Here we assume the wave amplitude is small so that nonlinear effects are negligible.

A. Sound propagation in media with space-time modulated density

We begin by considering a one-dimensional waveguide in which the effective density ρ of the medium is modulated in both space and time while bulk modulus remains constant. Generally, ρ is dispersive, i.e., $\rho = \rho(x, t, \omega)$. According to Newton's second law and Hooke's law,

$$\begin{aligned} -\frac{\partial p}{\partial x} &= \rho \frac{\partial v}{\partial t}, \\ -\frac{\partial p}{\partial t} &= \kappa \frac{\partial v}{\partial x}. \end{aligned} \tag{1}$$

Taking the partial derivative with respect to t and x, respectively, we get

$$\begin{aligned} -\frac{\partial^2 p}{\partial x \partial t} &= \frac{\partial \rho}{\partial t}\frac{\partial v}{\partial t} + \rho \frac{\partial^2 v}{\partial t^2}, \\ -\frac{\partial^2 p}{\partial x \partial t} &= \kappa \frac{\partial^2 v}{\partial x^2}. \end{aligned} \tag{2}$$

Combining the two equations to eliminate p, we can get the wave equation in the velocity, namely,

$$\frac{\partial^2 v}{\partial x^2} = \frac{1}{\kappa}\frac{\partial \rho}{\partial t}\frac{\partial v}{\partial t} + \frac{\rho}{\kappa}\frac{\partial^2 v}{\partial t^2} \tag{3}$$

Let us assume the solution is composed of two waves with different frequencies in the waveguide with the form

$$\begin{aligned} v_1 &= A_1(x)e^{j(\omega_1 t - k_1 x)}, \\ v_2 &= A_2(x)e^{j(\omega_2 t - k_2 x)}, \end{aligned} \tag{4}$$

where $k_1 = \frac{\omega_1}{c_1}$, $k_2 = \frac{\omega_2}{c_2}$, $c_1 = \sqrt{\frac{\kappa}{\rho_1}}$, and $c_2 = \sqrt{\frac{\kappa}{\rho_2}}$. The total wave velocity is given by $v = v_1 + v_2$.

Let us further assume that the density modulation is sufficiently weak that A_1 and A_2 are slowly varying and $\frac{\partial^2 A_{1,2}}{\partial x^2}$ are negligible. We assume the density variation is described by

$$\rho = \rho_1[1 + m_1 \cos(\Omega t - \beta x)] \tag{5}$$

for the wave with frequency ω_1 and

$$\rho = \rho_2[1 + m_2 \cos(\Omega t - \beta x)] \tag{6}$$

for the wave with frequency ω_2.

Typically, the density and bulk modulus are just fundamental properties of a material and are not a function of frequency. Therefore, the amplitude of variation remains constant for different frequencies, and hence, $m_1 = m_2$. However, for metamaterials, the effective density is controlled by the parameters of the metamaterial structure, such as the mass and in-plane tension for membranes, and the effective density is usually dispersive. Therefore, the modulation depth for different frequencies can be different. The quantities m_1 and m_2 represent the amplitude of effective density change for the corresponding frequencies when the controlling parameter changes, and it follows $m_1 = m_2$ in a nondispersive medium.

B. Unidirectional frequency conversion

The general space-time modulation described above admits a number of different types of solutions. We focus first on unidirectional frequency conversion. Here we define

$$\begin{aligned} \Omega &= \omega_1 - \omega_2, \\ \beta &= k_1 - k_2. \end{aligned} \tag{7}$$

Putting these into Eq. (3), we find that the two frequencies are coupled through the time-varying density $\rho(x, t, \omega)$. It can easily be shown that

$$\begin{aligned} &B_1 e^{j(\omega_1 t + k_1 x)}, B_2 e^{j(\omega_2 t + k_2 x)}, \\ &A_1^* e^{-j(\omega_1 t - k_1 x)}, A_2^* e^{-j(\omega_2 t - k_2 x)}, \\ &B_1^* e^{-j(\omega_1 t + k_1 x)}, B_2^* e^{-j(\omega_2 t + k_2 x)} \end{aligned} \tag{8}$$

are also coupled solutions. $A_1 e^{j(\omega_1 t - k_1 x)}$ is a forward-traveling wave, $B_1 e^{j(\omega_1 t + k_1 x)}$ is a backward-traveling wave, and $A_1^* e^{-j(\omega_1 t - k_1 x)}$ and $B_1^* e^{-j(\omega_1 t + k_1 x)}$ are their complex conjugates. The complete solution of Eq. (3) is composed of four mixed pairs. Without loss of generality, here for illustration we just analyze the first coupled pair. We put the form of assumed waves and prescribed modulation into Eq. (3), neglect the $\frac{\partial^2 A_{1,2}}{\partial x^2}$ terms, and equate the terms with the same frequency. The result is the following two equations:

$$\begin{aligned} \frac{\partial A_1}{\partial x} &= -j\frac{\rho_2 m_2}{4\kappa}\frac{\omega_1 \omega_2}{k_1}A_2, \\ \frac{\partial A_2}{\partial x} &= -j\frac{\rho_1 m_1}{4\kappa}\frac{\omega_1 \omega_2}{k_2}A_1. \end{aligned} \tag{9}$$

By taking the partial derivative and eliminating A_2, we get a partial differential equation for A_1:

$$\frac{\partial^2 A_1}{\partial x^2} = -\frac{m_1 m_2 k_1 k_2}{16}A_1. \tag{10}$$

Solving this equation yields

$$A_1 = a_1 e^{j\alpha x} + b_1 e^{-j\alpha x}, \tag{11}$$

where $\alpha = \frac{\sqrt{m_1 m_2 k_1 k_2}}{4}$ and a_1 and b_1 are constants decided by the boundary conditions. Putting the form of A_1 into Eq. (9)

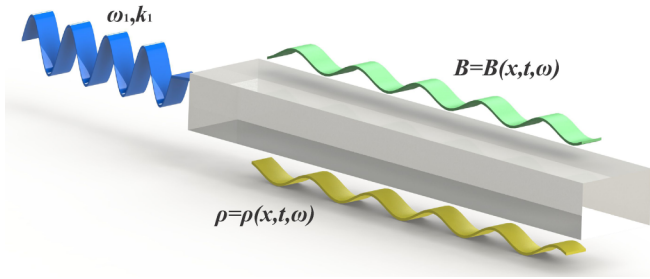

FIG. 1. Spatiotemporally modulated medium under study. The effective density or effective compressibility is dependent on time, space, and frequency.

to solve A_2, we get

$$A_2 = -\sqrt{\frac{m_1 k_1 \rho_1}{m_2 k_2 \rho_2}}(a_1 e^{j\alpha x} - b_1 e^{-j\alpha x}). \tag{12}$$

Therefore, we finally have the solution

$$v_1 = (a_1 e^{j\alpha x} + b_1 e^{-j\alpha x}) e^{j(\omega_1 t - k_1 x)},$$
$$v_2 = -\sqrt{\frac{m_1 k_1 \rho_1}{m_2 k_2 \rho_2}}(a_1 e^{j\alpha x} - b_1 e^{-j\alpha x}) e^{j(\omega_2 t - k_2 x)}. \tag{13}$$

Similar results can be found with other coupled pairs. If, at $x = 0$,

$$v_1(0,t) = a e^{j(\omega_1 t + \theta)},$$
$$v_2(0,t) = 0, \tag{14}$$

the complete solution to Eq. (3) is

$$v_1 = a\cos(\alpha x) e^{j(\omega_1 t - k_1 x + \theta)},$$
$$v_2 = -\sqrt{\frac{m_1 k_1 \rho_1}{m_2 k_2 \rho_2}}\, a \sin(\alpha x) e^{j(\omega_2 t - k_2 x + \theta + \frac{\pi}{2})}. \tag{15}$$

Therefore, the intensities of these two waves are

$$I_1 = \frac{1}{2}\rho_1 c_1 |v_1|^2 = \frac{1}{2} Z_1 a^2 \cos^2(\alpha x),$$
$$I_2 = \frac{1}{2}\rho_2 c_2 |v_2|^2 = \frac{1}{2} Z_2 \frac{m_1 k_1 \rho_1}{m_2 k_2 \rho_2} a^2 \sin^2(\alpha x), \tag{16}$$

where $Z_1 = \rho_1 c_1$ and $Z_2 = \rho_2 c_2$ are characteristic impedances of the two waves. The transfer factor is defined as the pressure amplitude of both modes over that of the incident mode,

$$\eta_1 = \frac{|v_1(x)|}{|v_1(0)|} = |\cos(\alpha x)|,$$
$$\eta_2 = \frac{|v_2(x)|}{|v_1(0)|} = \sqrt{\frac{m_1 k_1 \rho_1}{m_2 k_2 \rho_2}}\,|\sin(\alpha x)|. \tag{17}$$

From the plotted transfer factor in Fig. 2(a) we can see how the modes are transferred back and forth along the propagation. Equations (17) show that if we apply a signal of frequency ω_1 at the input end of the waveguide, the power at that frequency is completely converted to that of ω_2 over a distance of $\alpha x = \frac{\pi}{2}$. In the next segment of length $\alpha x = \frac{\pi}{2}$, the power of frequency ω_2 reverts to that of ω_1 and then converts back and forth. At $\alpha x = 0, \pi, 2\pi, \ldots$, $|I_1|$ is at maximum, and at

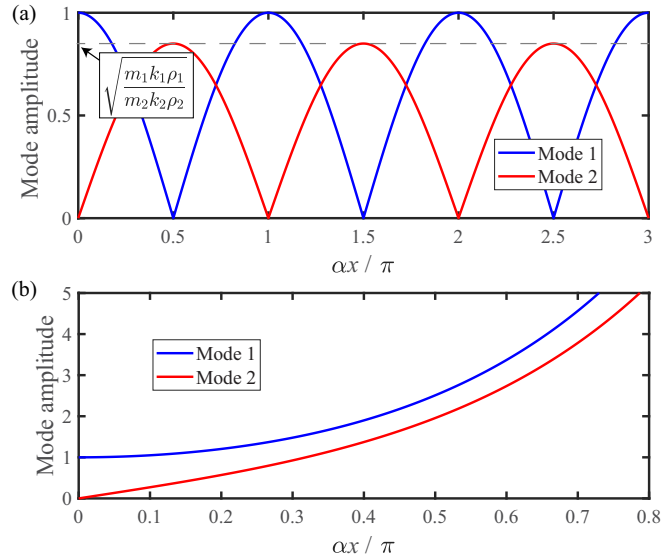

FIG. 2. Transfer factor between the two modes as the sound propagates in the space-time modulated waveguide. (a) The energy converts back and forth between the two modes. (b) In the case of parametric amplification, the two coupled modes both grow exponentially.

$\alpha x = \pi/2, 3\pi/2, 5\pi/2, \ldots$, $|I_2|$ is at maximum. On the other hand, the backward-propagating wave will not be affected since the generated mode is not supported in such a system.

C. Unidirectional parametric amplification and phase conjugation

Another class of solution enabled by space-time modulation is parametric amplification, where the incident wave is amplified exponentially while propagating in such media. We begin by defining

$$\Omega = \omega_1 + \omega_2,$$
$$\beta = k_1 + k_2; \tag{18}$$

then the two coupled waves become

$$v_1 = A_1(x) e^{j(\omega_1 t - k_1 x)},$$
$$v_2 = A_2(x) e^{-j(\omega_2 t - k_2 x)}. \tag{19}$$

Inserting these into Eq. (3) and going through a similar process, we can find that the governing equation for A_1 becomes

$$\frac{\partial^2 A_1}{\partial x^2} = \frac{m_1 m_2 k_1 k_2}{16} A_1 \tag{20}$$

and the solution for A_1 and A_2 yields

$$A_1 = a_1 e^{\alpha x} + b_1 e^{-\alpha x},$$
$$A_2 = -j\sqrt{\frac{m_1 k_1 \rho_1}{m_2 k_2 \rho_2}}(a_1 e^{\alpha x} - b_1 e^{-\alpha x}), \tag{21}$$

where $\alpha = \frac{\sqrt{m_1 m_2 k_1 k_2}}{4}$. Applying the same boundary conditions as for Eq. (14), we get the complete solution of Eq. (3) as

$$v_1 = a\frac{e^{\alpha x} + e^{-\alpha x}}{2} e^{j(\omega_1 t - k_1 x + \theta)},$$
$$v_2 = \sqrt{\frac{m_1 k_1 \rho_1}{m_2 k_2 \rho_2}} a \frac{e^{\alpha x} - e^{-\alpha x}}{2} e^{-j(\omega_2 t - k_2 x - \theta + \frac{\pi}{2})}. \quad (22)$$

The transfer factors are

$$\eta_1 = \frac{|v_1(x)|}{|v_1(0)|} = \frac{e^{\alpha x} + e^{-\alpha x}}{2},$$
$$\eta_2 = \frac{|v_2(x)|}{|v_1(0)|} = \sqrt{\frac{m_1 k_1 \rho_1}{m_2 k_2 \rho_2}} \frac{e^{\alpha x} - e^{-\alpha x}}{2}. \quad (23)$$

Now, instead of periodically varying, the amplitudes of both waves are growing exponentially, as shown in Fig. 2(b). In this way we can get a piece of "gain" material for both frequencies. A special case is that when $\omega_1 = \omega_2$, both waves have the same frequency. In this case, there will be two waves at the output end: one is the amplified original wave, and the other one is the generated wave with the same frequency but with conjugated phase plus a certain phase delay.

Here we have shown two possibilities enabled by space-time modulation as described in Eqs. (7) and (18), namely, unidirectional frequency conversion and parametric amplification, which cannot easily be realized in reciprocal systems. However, we would like to emphasize that these are just two classes of solutions of a space-time modulated system, and there are many more possibilities depending on the modulation strategy.

D. Sound propagation in media with a space-time modulated bulk modulus

Similar to the case with modulated density, a waveguide with a space-time modulated bulk modulus can also produce nonreciprocal one-way wave behaviors such as frequency conversion, amplification, and phase conjugation. We will show that the solutions will have a similar structure but different scaling constants. The wave equation in such a medium is written as

$$-\frac{\partial p}{\partial x} = \rho \frac{\partial v}{\partial t},$$
$$-\frac{\partial (Bp)}{\partial t} = \frac{\partial v}{\partial x}, \quad (24)$$

where $B = \frac{1}{\kappa}$ is the compressibility (or effective compressibility) of the medium under study. With these two equations, the wave equation can be obtained in the form of

$$\frac{\partial^2 p}{\partial x^2} = \rho \frac{\partial^2 B}{\partial t^2} p + 2\rho \frac{\partial B}{\partial t}\frac{\partial p}{\partial t} + \rho B \frac{\partial^2 p}{\partial t^2}. \quad (25)$$

Suppose the compressibility of the medium in the waveguide is varying with the form

$$B = B_1[1 + m_1 \cos(\Omega t - \beta x)] \quad (26)$$

for the wave with frequency ω_1 and

$$B = B_2[1 + m_2 \cos(\Omega t - \beta x)] \quad (27)$$

for the wave with frequency ω_2 and the solution has the form of $p = p_1 + p_2$, where

$$p_1 = A_1(x) e^{j(\omega_1 t - k_1 x)},$$
$$p_2 = A_2(x) e^{j(\omega_2 t - k_2 x)}. \quad (28)$$

For frequency conversion we can apply the modulation in the same form as in Eqs. (10) and (11). Putting it in Eq. (25) and equating the terms with the same frequency and wave number, we can get the same differential equation for A_1 as in Eq. (10). Solving A_1 and A_2, we get

$$A_1 = a_1 e^{j\alpha x} + b_1 e^{-j\alpha x},$$
$$A_2 = -\frac{B_1}{B_2}\sqrt{\frac{m_1 k_2}{m_2 k_1}}(a_1 e^{j\alpha x} - b_1 e^{-j\alpha x}), \quad (29)$$

where $\alpha = \frac{\sqrt{m_1 m_2 k_1 k_2}}{4}$. Applying the boundary condition at $x = 0$,

$$p_1(0, t) = a e^{j(\omega_1 t + \theta)},$$
$$p_2(0, t) = 0, \quad (30)$$

the following complete solution can be found:

$$p_1 = a\cos(\alpha x) e^{j(\omega_1 t - k_1 x + \theta)},$$
$$p_2 = -\frac{B_1}{B_2}\sqrt{\frac{m_1 k_2}{m_2 k_1}} a \sin(\alpha x) e^{j(\omega_2 t - k_2 x + \theta + \frac{\pi}{2})}. \quad (31)$$

The transfer factors become

$$\eta_1 = \frac{|p_1(x)|}{|p_1(0)|} = |\cos(\alpha x)|,$$
$$\eta_2 = \frac{|p_2(x)|}{|p_1(0)|} = \frac{B_1}{B_2}\sqrt{\frac{m_1 k_2}{m_2 k_1}} |\sin(\alpha x)|. \quad (32)$$

Similarly, if the applied modulation is the same as in Eq. (18), parametric amplification and phase conjugation can be achieved. The transfer factors for mode conversion and parametric amplification have the same form as in Fig. 2 with different amplitudes. From Eq. (31) we can see that Manley-Rowe relations [47] do not apply due to the dispersion of the metamaterial. However, if we reduce the model to a nondispersive material by enforcing $B_1 = B_2$, $c_1 = c_2$, and $m_1 = m_2$, the Manley-Rowe relations will be satisfied.

III. METAMATERIAL REALIZATION OF SPACE-TIME MODULATED ACOUSTIC MEDIA

In some cases, for elastic waves in solids, material properties can be tuned by an external field. For example, one can change the elastic modulus by applying a voltage to a piece of piezoelectric material. However, directly changing the properties of a fluid is challenging since modulating density or bulk modulus usually means modulating the temperature in a fast and controlled manner. In recent years, the development of the concept of metamaterials has enabled theoretically arbitrary values of effective density or modulus by carefully designing the subwavelength structures of the material [48,49].

By introducing active elements into the metamaterials, the achieved values can further be controlled. It opens up the

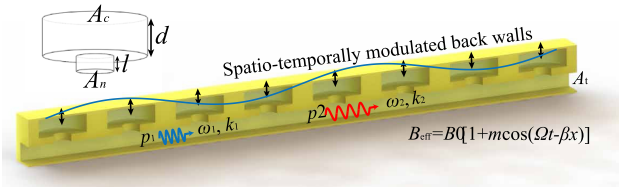

FIG. 3. One proposed realization of a space-time modulated acoustic wave system. The moving back wall allows the cavity volume to be modulated. The inset shows the dimensions of a single Helmholtz resonator.

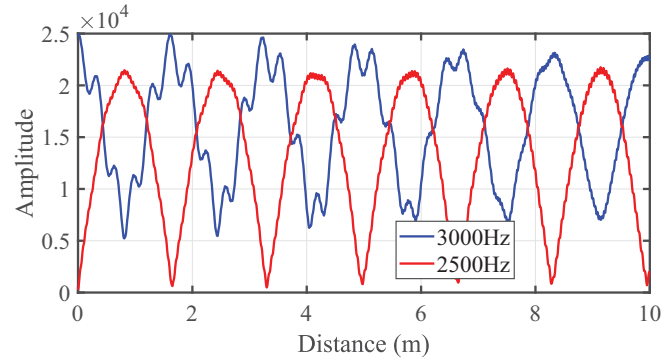

FIG. 4. Two targeted frequency components along the space-time modulated media in the FDTD simulation. The wave energy transfers back and forth between the two components.

possibility to manipulate the effective parameters spatiotemporally without too much cost to achieve enough modulation depth at the desired rate. Piezoelectric membranes, for example, have been proposed for tuning the effective density to change the working frequency [50,51]. However, such membranes can achieve only limited tunability at the cost of extremely high voltages, and it is hard to modulate dynamically. Here we propose the dynamic change in a system with an array of side-loaded Helmholtz resonators, in which the effective bulk modulus can be modulated through small motion of the back walls, as shown in Fig. 3.

The effective compressibility for a metamaterial system composed of static resonators can be written as [52,53]

$$B_{\text{eff}}(\omega) = B_0\left[1 + \frac{F\omega_0^2}{\omega_0^2 - \omega^2 + j\omega\gamma}\right], \tag{33}$$

where $F = nA_c d/A_t$ is the geometrical factor, n is the number of cells per meter, A_c is the area of the cavity back wall, d is the height of the cavity, and A_t is the cross-sectional area of the waveguide. The parameter $\omega_0^2 = \frac{c_0^2 A_n}{A_c d l}$ is the resonant angular frequency, where A_n is the cross-sectional area of the neck and l is the corrected length of the neck. The factor $\gamma = \frac{R}{\rho_0 A_n l}$, where R is associated with the thermal viscous loss in the neck region. In general, γ is affected by the frequency, air viscosity, shape of the neck, and roughness of the surface of the fabricated structure. In practice, γ is usually estimated by measuring the effective material properties and fitting the experimental data to the theoretical model [52].

We now consider a metamaterial in which the back wall of the cavity is moving sinusoidally so that d changes with time as $d = d + \delta d\cos(\Omega t - \beta x)$. We can rewrite the effective compressibility as

$$B_{\text{eff}}(\omega, d) = B_0 + \frac{\frac{nA_n}{A_t l \rho_0}}{\frac{c_0^2 A_n}{A_c l d} - \omega^2 + j\omega\gamma}. \tag{34}$$

Assuming weak modulation, the modulation depth m at a given frequency can be estimated with

$$m(\omega) = \frac{|\text{Re}[B_{\text{eff}}(\omega, d+\delta d)] - \text{Re}[B_{\text{eff}}(\omega, d-\delta d)]|}{2\text{Re}[B_{\text{eff}}(\omega, d)]}. \tag{35}$$

The wave number of the system can be calculated with $k(\omega) = \omega\sqrt{B_{\text{eff}}(\omega)\rho_0}$. Hence, for a given system and the targeted frequencies ω_1 and ω_2, the wave numbers k_1 and k_2 can be calculated, and the corresponding modulation depth at both frequencies can be estimated with Eq. (35). Then the rate of mode conversion and parametric amplification can be estimated by calculating α in Eqs. (11), (12), (21), and (29). The length of space-time modulated metamaterial can then be determined according to the target applications.

IV. NUMERICAL SIMULATIONS

The analytical model is verified here with a one-dimensional FDTD effective-medium simulation. The background medium is lossless air with density $\rho_0 = 1.2$ kg/m^3 and speed of sound $c_0 = 343$ m/s. The time step is 2×10^{-6} s, and the grid is 1×10^{-3} m. In the simulation, we study the wave propagation in an effective-medium approximation of the metamaterial structure with modulated cavity height, as described in Sec. III. The number of resonators is $n = 25$ m^{-1}. The round necks have a radius of 5 mm and corrected length $l = 6$ mm, and the cavity is a cylinder with a radius of 14 mm and height $d = 4$ mm, so that the resonant frequency is 3980 Hz. The modulation depth is $\delta d = 0.4$ mm. The wave propagates in a nonmodulated medium before (upstream) and after (downstream) the modulated section. A sinusoidal wave is incident from the upstream direction. To show that the wave interacts differently with the space-time modulation in different directions, we simulate the wave incident from both directions. The backward incident wave was simulated by switching the sign of the modulation wave number to $-\beta$.

We first simulate the wave propagation in a modulated medium where the modulation satisfies Eq. (7), so that the device acts as a frequency converter. The target input and output frequencies are $f_1 = 3000$ Hz and $f_2 = 2500$ Hz, respectively. The modulated length is 10 m, with an upstream length of 0.3 m and a downstream length of 30 m, so that the reflection from the boundary can be easily time gated. To study the steady-state wave behavior, the data from the first 80 ms are excluded from processing. The simulated pressure field in the modulated region is recorded for 100 ms after the signals reach the steady state. Figure 4 shows the amplitude of the two frequency components along the modulated medium. From Fig. 4 we clearly see that the wave energy gradually shifts from f_1 to f_2 and then transfers back to f_1, as predicted in the theory. The distance for f_2 to get to its first peak is 0.81 m in the simulation, while the corresponding theoretical calculation is 0.78 m, in good agreement. The small discrepancy

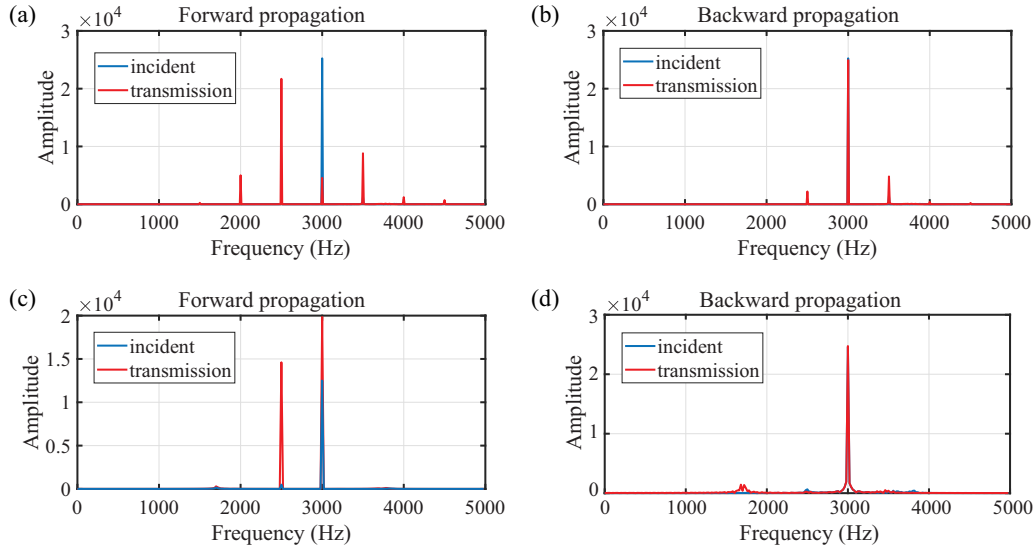

FIG. 5. Simulated spectrum of the incident and transmitted waves when the device is modulated as a frequency converter or parametric amplifier for both directions. (a) Frequency converter; the wave is converted from f_1 to f_2 while propagating in the positive direction. (b) When it is propagating in the negative direction, it does not interact with the modulation, so that the transmitted wave is almost the same as the incident wave. (c) Parametric amplifier; f_1 got amplified in the positive direction, generating f_2 in the meantime. (d) The wave is not affected while propagating in the negative direction.

originates from the finite resolution in the simulation. We can see small oscillations in the curve for 3000 Hz, which gradually fade out with distance. This is because in the simulation, the wave is incident from a stationary medium into a space-time-varying medium. As reflections from the boundary, especially the higher-order waves, will perturb the fundamental model, there are small oscillations near the interface. These perturbations will gradually disappear as they propagate away from the edge, and the wave behavior meets the expectation from the theory, as can be seen in Fig. 4.

An advantage of the proposed metamaterial implementation of an acoustic space-time modulated medium lies in the fact that all the different functionalities can be achieved without changing the structure of the system, and the behavior depends only on how the resonators are modulated. For the functionalities described in Sec. II, the corresponding simulation results are summarized in Fig. 5. For the frequency converter, the target input and output frequencies are $f_1 = 3000$ Hz and $f_2 = 2500$ Hz, respectively. The signals on the incident side and the transmission side of the modulated medium were recorded for analysis. Figures 5(a) and 5(b) show the spectrum of the incident wave and transmitted wave when the wave is incident from the positive direction and the negative direction, respectively. From Figs. 5(a) and 5(b) we can see that for the wave incident from the positive direction, the main frequency component is effectively converted from 3000 to 2500 Hz. The wave incident from the negative direction is not significantly affected by the modulation.

For nonreciprocal one-way wave transmission at 3000 Hz, the isolation level measures the efficiency of one-way isolation of the acoustic waves, defined as the contrast between the transmission coefficient amplitudes for each frequency when the wave is incident from opposite directions. Although the isolation level can theoretically reach infinity, in the simulation, it reaches 13 dB. This is due to the incomplete conversion between two waves and conversion to other frequency components. If we look at 2500 Hz, then the isolation level reaches 26 dB in simulation. To study the effect of the modulation depth on the observed nonreciprocity, we sweep the modulation depth m from 1% to 20% in the simulation at a step of 0.2%, and the change in isolation level is shown in Fig. 6. Note here that as modulation changes, the distance required for total conversion also changes, as can be seen from Eq. (17) . Counterintuitively, the isolation level can be increased with a smaller modulation depth, which is because of the better approximation to the weak-modulation assumption in our derivation. For example, when modulation depth $m = 1\%$ is applied ($\delta d = 0.04$ mm), the isolation level for 3000 and 2500 Hz reaches 48 and 44 dB, respectively. However, as a trade-off, lower modulation depth would result in a longer system. We can see some oscillations in the isolation level as the modulation depth changes. But they do not affect the

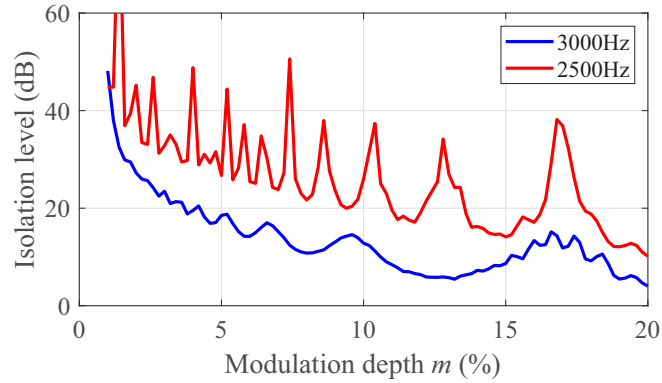

FIG. 6. Change in the isolation level for both 3000- and 2500-Hz waves as the modulation depth varies. Counterintuitively, a higher isolation level is achieved with a smaller modulation depth.

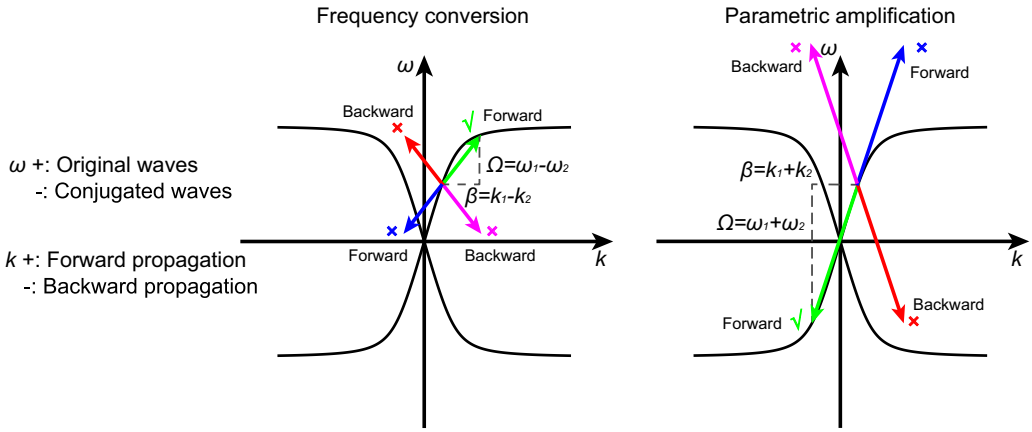

FIG. 7. Modulation facilitates mode hopping on the ω-k diagram. Only supported modes of the system can be coupled through modulation. This feature allows one-way manipulation of waves.

main conclusions in this paper. The physical origin of these oscillations, on the other hand, would be an interesting topic for further investigation.

To study the system's robustness against losses in the resonators, we have also simulated the system with embedded loss by assigning γ in Eq. (33) different values ranging from 0 to $0.02\omega_1$, and the isolation level remains essentially unchanged. The isolation level is 10 to 13 dB for 3000 Hz and remains 26 dB for 2500 Hz within the range. Note here that by assigning different values of loss from 0 to $0.02\omega_1$, the ω-k diagram of the waveguide is changed accordingly; therefore, the length of the modulated section is also adjusted. This feature makes the whole system robust against losses in real implementations. However, as the loss increases, the insertion loss will increase, which will decrease the transmission amplitude for both frequencies.

If the device is modulated according to the space-time profile of Eq. (18), it acts as a parametric amplifier. Both f_1 (3000 Hz) and f_2 (2500 Hz) grow exponentially. The simulated spectrum on the incident side and transmission side is shown in Fig. 5(c). In the simulation, the modulated length is 0.5 m to prevent the signals from growing too large. Upstream length is 5 m, while downstream length is 20 m to prevent reflection. The modulation depth remains unchanged. From Fig. 5(c) it is seen that as the incident wave propagates in the space-time modulated media, the waves get amplified while generating the other frequency component. The growth rate α can be calculated by taking the amplitude ratio between the incident f_1 and the generated f_2 and then solving Eq. (22). The calculated growth rates from the simulated result and theoretical calculation are $\alpha = 1.9917$ and $\alpha = 2.0082$, respectively, which again show excellent agreement between the theory and simulation. Figure 5(d) shows the wave propagating in the negative direction. We can see that the wave is not affected by the modulation. Therefore, the device facilitates one-way parametric amplification.

To understand the physical mechanism of the proposed system, the corresponding one-way phenomena can be viewed as a mode conversion on the ω-k diagram, which corresponds to the interband and intraband photon transition in optical systems, as shown in Fig. 7. It is shown that the two otherwise orthogonal modes are coupled through the modulation. However, the wave will not interact with the modulation if the modulation does not lead to any mode that is allowed in the system. Therefore, the prescribed modulation works only for the forward-propagating wave, as shown in Fig. 5. For each type of modulation, the green and blue arrows denote the modulation when the wave travels in the forward direction, while the red and magenta arrows denote the modulation when the wave travels in the backward direction. In the diagram we see that only the designed mode is coupled through modulation. This is analogous to the mechanism of modulated phononic crystals in the mass-spring systems [36–38].

Since the modulation relies on shifting of the ω-k diagram, it is important to avoid coupling to unwanted modes for efficient spectral manipulation. For example, if the material has a purely linear ω-k diagram, the modes with $\omega = \omega_1 \pm n\Omega$ will all be coupled, and all of these coupling terms need to be taken into consideration in the theory. Due to the dispersive nature of metamaterials, coupling between higher-order modes will not be matched with the modulation strategy. Therefore, space-time modulation of the metamaterials provides an advantage over conventional modulated transmission lines, where waves of all frequencies share the same velocity. By carefully designing a system with specific ω-k relationships and optimizing the modulation strategy to avoid unwanted coupling, better control over the spectrum can be achieved. Also, since the theory in this paper describes space-time modulation of a discretized effective medium, finer discretization can better mimic a continuous medium, and thus the theoretical calculation of the ω-k diagram would be more accurate. However, we would also like to note that the modulation strategy here is determined by the frequencies and wave numbers of the targeting modes that can be read off from the ω-k diagram. Changing the spacing between resonators will also change the resulting dispersion relation, and the modulation strategy can be adjusted to accommodate these changes as long as the homogenization of the metamaterial is valid.

V. SUMMARY AND CONCLUSIONS

Here we have developed a theory to characterize the waves propagating in an acoustic space-time modulated medium. Specifically, when the medium is modulated such that

different modes can be coupled through that modulation, nonreciprocal functionalities such as one-way frequency conversion and parametric amplification can be achieved, which is beyond the reach of linear time-invariant systems. We showed how such a medium could be implemented using small structural modulation of Helmholtz resonators, and a numerical FDTD simulation based on such a design was developed to show that the theory is valid and that the predicted behavior can be delivered in practice. The simulation results showed excellent agreement with theoretical calculations.

Our work outlines a robust and efficient means of versatile manipulation of an incident wave compared with nonlinear devices which can generate only harmonics of the fundamental mode and in which there is little control over the ratio between the fundamental mode and its harmonics. Compared with conventional time-varying transmission lines, introducing dispersion into space-time modulated media decouples the higher-order modes with modulation, which helps prevent generation of higher-order modes. Also, since the device does not require operation near resonant frequencies, it is less sensitive to losses and fabrication errors, which provides a significant advantage in realization compared with nonreciprocal devices based on coupled resonances. Furthermore, the loss in the resonators can be compensated by the modulation strategy, so that the nonreciprocal wave transport is immune to the inherent losses in the resonators. It is also noted that the modulation is determined by the ω-k relationship, regardless of the structures that we use for realization. Therefore, it can also be realized with other types of metamaterial structures.

The mode conversion process mediated by the frequency and momentum of the modulation is an "indirect phononic transition," in analogy with indirect electronic transitions in semiconductors, where interaction with optical signals and phonons changes the energy and momentum of electrons. Here we offered a perspective on solving space-time equations directly instead of analyzing band structures with Floquet theory. It provides more detailed information about how waves change gradually in such systems. These nonreciprocal phenomena open many possibilities for unprecedented wave control capability. For example, mode conversion enables advanced spectrum control for one-way and encoded communications, directional energy transmission control, and directional band gap for acoustic rectifiers and topological insulators; parametric amplification provides a possible way for designing the gain media in parity-time-symmetric systems and powerful acoustic radiator designs; and phase conjugation enables all-angle retroreflectors, acoustic lasing, and mathematical operation for data processing and may find applications in acoustic communication systems.

ACKNOWLEDGMENTS

This work was supported by a Multidisciplinary University Research Initiative grant from the Office of Naval Research (Grant No. N00014-13-1-0631) and an Emerging Frontiers in Research and Innovation grant from the National Science Foundation (Grant No. 1641084).

[1] J. D. Adam, L. E. Davis, G. F. Dionne, E. F. Schloemann, and S. N. Stitzer, IEEE Trans. Microwave Theory Tech. **50**, 721 (2002).
[2] D. L. Sounas and A. Alú, Phys. Rev. Lett. **118**, 154302 (2017).
[3] D. L. Sounas, J. Soric, and A. Alù, Nat. Electron. **1**, 113 (2018).
[4] D. L. Sounas, C. Caloz, and A. Alù, Nat. Commun. **4**, 2407 (2013).
[5] M. C. Rechtsman, J. M. Zeuner, Y. Plotnik, Y. Lumer, D. Podolsky, F. Dreisow, S. Nolte, M. Segev, and A. Szameit, Nature (London) **496**, 196 (2013).
[6] L. Lu, J. D. Joannopoulos, and M. Soljačić, Nat. Photonics **8**, 821 (2014).
[7] A. B. Khanikaev and G. Shvets, Nat. Photonics **11**, 763 (2017).
[8] R. Fleury, D. Sounas, M. R. Haberman, and A. Alù, Acoust. Today **11**, 14 (2015).
[9] B. Liang, B. Yuan, and J.-C. Cheng, Phys. Rev. Lett. **103**, 104301 (2009).
[10] B. Liang, X. Guo, J. Tu, D. Zhang, and J. Cheng, Nat. Mater. **9**, 989 (2010).
[11] N. Boechler, G. Theocharis, and C. Daraio, Nat. Mater. **10**, 665 (2011).
[12] B.-I. Popa and S. A. Cummer, Nat. Commun. **5**, 3398 (2014).
[13] R. Fleury, D. L. Sounas, C. F. Sieck, M. R. Haberman, and A. Alù, Science **343**, 516 (2014).
[14] Z. Yang, F. Gao, X. Shi, X. Lin, Z. Gao, Y. Chong, and B. Zhang, Phys. Rev. Lett. **114**, 114301 (2015).
[15] X. Ni, C. He, X.-C. Sun, X.-p. Liu, M.-H. Lu, L. Feng, and Y.-F. Chen, New J. Phys. **17**, 053016 (2015).
[16] R. Fleury, A. B. Khanikaev, and A. Alù, Nat. Commun. **7**, 11744 (2016).
[17] Y. Ding, Y. Peng, Y. Zhu, X. Fan, J. Yang, B. Liang, X. Zhu, X. Wan, and J. Cheng, Phys. Rev. Lett. **122**, 014302 (2019).
[18] P. Tien and H. Suhl, Proc. IRE **46**, 700 (1958).
[19] P. Tien, J. Appl. Phys. **29**, 1347 (1958).
[20] A. Cullen, Nature (London) **181**, 332 (1958).
[21] J.-C. Simon, IRE Trans. Microwave Theory Tech. **8**, 18 (1960).
[22] A. Oliner and A. Hessel, IRE Trans. Microwave Theory Tech. **9**, 337 (1961).
[23] E. Cassedy and A. Oliner, Proc. IEEE **51**, 1342 (1963).
[24] E. Cassedy, Proc. IEEE **55**, 1154 (1967).
[25] C. Elachi, IEEE Trans. Antennas Propag. **20**, 534 (1972).
[26] S. Qin, Q. Xu, and Y. E. Wang, IEEE Trans. Microwave Theory Tech. **62**, 2260 (2014).
[27] C. G. Poulton, R. Pant, A. Byrnes, S. Fan, M. Steel, and B. J. Eggleton, Opt. Express **20**, 21235 (2012).
[28] M. Hafezi and P. Rabl, Opt. Express **20**, 7672 (2012).
[29] D. L. Sounas and A. Alú, ACS Photonics **1**, 198 (2014).
[30] Y. Hadad, D. L. Sounas, and A. Alu, Phys. Rev. B **92**, 100304(R) (2015).
[31] D. Correas-Serrano, J. Gomez-Diaz, D. Sounas, Y. Hadad, A. Alvarez-Melcon, and A. Alù, IEEE Antennas Wireless Propag. Lett. **15**, 1529 (2016).

[32] F. Ruesink, M.-A. Miri, A. Alù, and E. Verhagen, Nat. Commun. **7**, 13662 (2016).
[33] Y. Hadad, J. C. Soric, and A. Alu, Proc. Natl. Acad. Sci. USA **113**, 3471 (2016).
[34] S. Taravati and C. Caloz, IEEE Trans. Antennas Propag. **65**, 442 (2017).
[35] M.-A. Miri, F. Ruesink, E. Verhagen, and A. Alù, Phys. Rev. Appl. **7**, 064014 (2017).
[36] G. Trainiti and M. Ruzzene, New J. Phys. **18**, 083047 (2016).
[37] H. Nassar, H. Chen, A. Norris, M. Haberman, and G. Huang, Proc. R. Soc. A **473**, 20170188 (2017).
[38] Y. Wang, B. Yousefzadeh, H. Chen, H. Nassar, G. Huang, and C. Daraio, Phys. Rev. Lett. **121**, 194301 (2018).
[39] R. Fleury, D. L. Sounas, and A. Alù, Phys. Rev. B **91**, 174306 (2015).
[40] T. T. Koutserimpas and R. Fleury, Wave Motion **89**, 221 (2019).
[41] G. Floquet, Ann. Sci. Ec. Norm. Super., Ser. 2 **12**, 47 (1883).
[42] M. B. Zanjani, A. R. Davoyan, N. Engheta, and J. R. Lukes, Sci. Rep. **5**, 9926 (2015).
[43] X. Zhu, H. Ramezani, C. Shi, J. Zhu, and X. Zhang, Phys. Rev. X **4**, 031042 (2014).
[44] A. Brignon and J.-P. Huignard, *Phase Conjugate Laser Optics* (Wiley, Hoboken, NJ, 2003).
[45] G. S. He, Prog. Quantum Electron. **26**, 131 (2002).
[46] A. P. Brysev, L. Krutyanskii, and V. L. Preobrazhenskii, Phys. Usp. **41**, 793 (1998).
[47] J. Manley and H. Rowe, Proc. IRE **44**, 904 (1956).
[48] S. A. Cummer, J. Christensen, and A. Alù, Nat. Rev. Mater. **1**, 16001 (2016).
[49] G. Ma and P. Sheng, Sci. Adv. **2**, e1501595 (2016).
[50] G. Ma, M. Yang, S. Xiao, Z. Yang, and P. Sheng, Nat. Mater. **13**, 873 (2014).
[51] S. Xiao, G. Ma, Y. Li, Z. Yang, and P. Sheng, Appl. Phys. Lett. **106**, 091904 (2015).
[52] N. Fang, D. Xi, J. Xu, M. Ambati, W. Srituravanich, C. Sun, and X. Zhang, Nat. Mater. **5**, 452 (2006).
[53] S. H. Lee, C. M. Park, Y. M. Seo, Z. G. Wang, and C. K. Kim, J. Phys.: Condens. Matter **21**, 175704 (2009).